

Quantitative Lattice Simulations of the Structure and Thermodynamics of Macromolecules

Ananth Indrakanti and Janna K. Maranas

Department of Chemical Engineering, Pennsylvania State University, University Park, Pennsylvania 16802

Athanassios Z. Panagiotopoulos

Department of Chemical Engineering, Princeton University, Princeton, New Jersey 08540

Sanat K. Kumar*

Department of Materials Science and Engineering, Pennsylvania State University, University Park, Pennsylvania 16802

Received August 1, 2001

Revised Manuscript Received October 12, 2001

While there have been rapid advances in the efficiency of molecular simulations, there remain practically important problems which are outside the realm of current methods. For example, available methods can only be used for the simulation of the phase behavior of short-chain alkanes (i.e., $N \sim 50$) while accurately accounting for their structure and interactions.¹ Thus, the industrially important problem of polymer–polymer phase separation, which occurs only for $N > 200$ in the prototypical blend of polyethylene and polypropylene,² remains currently inaccessible by simulation. Standard, Ising-type lattice models can be used to simulate the phase behavior of truly long chains, e.g., $N = 10\,000$.³ However, since the chemical details of the molecules are ignored in these coarse-grained simulations, it is hard to relate them to the behavior of real polymers.

In contrast to these ideas, we have recently shown that finely discretized lattice models can quantitatively reproduce the off-lattice phase behavior and structure of *atomic* fluids, e.g., Lennard-Jones fluids and the restricted primitive model.^{4,5} In these cases each molecule occupies more than one lattice site, and we have empirically found that the ratio of the monomer diameter to the lattice size, ζ , must be greater than 5 to get quantitative agreement with off-lattice results. (In the same language a single precision computer, where position cannot be specified to better than seven significant figures, corresponds to a $\zeta \sim 10^7$ lattice.) Our work goes beyond past ideas of using discretization of free space as a computational tool, e.g., using the bond fluctuation model, since we have been able to *quantitatively* reproduce off-lattice results using the same potential model in both cases. Simulations on finely discretized lattices are computationally efficient due to the use of look-up tables for interaction energies. Thus, a speed-up of 10 for the enumeration of the gas–liquid coexistence for a Lennard-Jones fluid,⁵ and 100 for a model ionic fluid, over their corresponding off-lattice analogues have been reported.⁴

At this time it is unclear whether these ideas can be extended to molecular systems, such as polyolefins, which incorporate geometric constraints and also different moieties (methyl, methylene, and methyne). We utilize available off-lattice force fields for *n*-alkanes on

a finely grained lattice (typically $\zeta = 12$) and calculate the liquid–vapor coexistence curve, the distribution of torsional angles, and the intermolecular pair distribution function, $g(r)$, for chains $N \leq 100$. The fine-grained approaches *quantitatively reproduce* the off-lattice behavior for chain lengths simulated to date, i.e., $N \leq 48$,^{1,6} with speed-ups of 1 order of magnitude. Further, we report the first phase diagrams for chains of $N = 100$, thus showing that these methods can begin to access the true macromolecular limit. Finally, we derive the minimum ζ values necessary to reproduce the off-lattice behavior of atomic and polymeric fluids.

We utilize the united atom description for hydrocarbon chains, i.e., where each carbon atom and the hydrogen atoms bonded to it are treated as a single unit. All inter- and intramolecular interactions are described by the NERD potential.¹ In this model the bond length between adjacent united atoms is fixed at 1.54 Å, and bond bending is described through a stiff potential with an equilibrium bond angle of $\theta = 114^\circ$. The Lennard-Jones potential is used to describe nonbonded interactions, and the σ and ϵ parameters for the CH_2 (middle monomers) and CH_3 (chain end) moieties are different. The *only* simplification we make when this model is used on a lattice is to fix the bond angle at its equilibrium value, and we shall show that this assumption does not affect the quality of our phase equilibrium results. However, it has a measurable, but small, effect on the derived structural information. By picking the lattice size $a = 0.77$ Å, we can simultaneously accommodate the bond length constraint for ethane and get a large enough $\zeta \equiv \sigma/a \approx 5$ to properly model the dispersive interactions.^{4,5} (σ is the diameter of a methyl group.) For all the higher alkanes a smaller lattice size of $a = 0.308$ Å ($\zeta \sim 12$) is required to accommodate the bond length and angle constraints. We compute and tabulate the interactions between different moieties on this lattice explicitly using the appropriate σ and ϵ parameters for each pair. The interactions were truncated at $r = 13.86$ Å, and all properties corrected for long-range interactions.⁷

The gas–liquid coexistence of these alkanes were enumerated by the histogram reweighting method.^{4,8–15} Guided by ref 15, we performed a series of grand canonical Monte Carlo simulations with a fixed value of T and μ in each one and used only chain insertions and deletions as elementary Monte Carlo moves. The probability of the acceptance of these whole chain moves are enhanced through the use of the configurational bias method.¹⁶ Figure 1 shows that these lattice models quantitatively reproduce the off-lattice vapor–liquid coexistence curves for all of the hydrocarbons simulated to date, i.e., $N \leq 48$. The critical temperatures obey the Schulz–Flory law;¹⁷ i.e., a plot of $1/T_c$ vs $[1/\sqrt{N} + 1/(2N)]$ is linear for all $N > 10$. This gives us confidence in the estimated phase diagram for the $N = 100$, whose behavior has not been measured or simulated previously.

We also calculate the intermolecular pair distribution function, $g(r)$, and the distribution of torsional angles. These results, which were obtained by calculations in the canonical ensemble, are compared to molecular dynamics calculations using the same potential for C_{31} chains at liquidlike densities (0.7307 g/cm^3) at

* Corresponding author: E-mail kumar@plmsc.psu.edu.

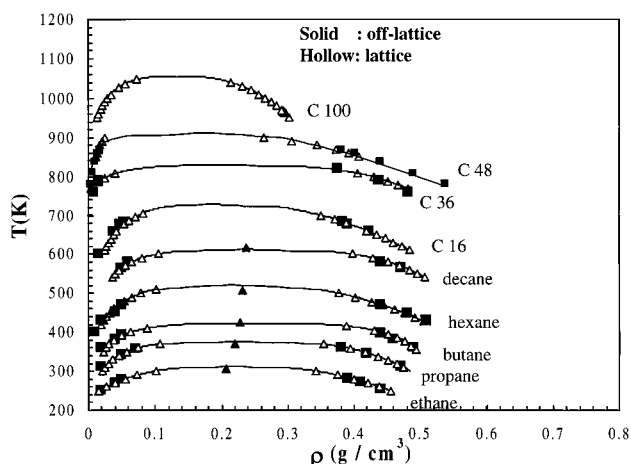


Figure 1. Comparison of liquid–gas phase coexistence for pure *n*-alkanes as obtained from lattice simulations to published off-lattice results from ref 1. The filled triangles are experimental critical points, while the lines are fits to Ising scaling ideas.

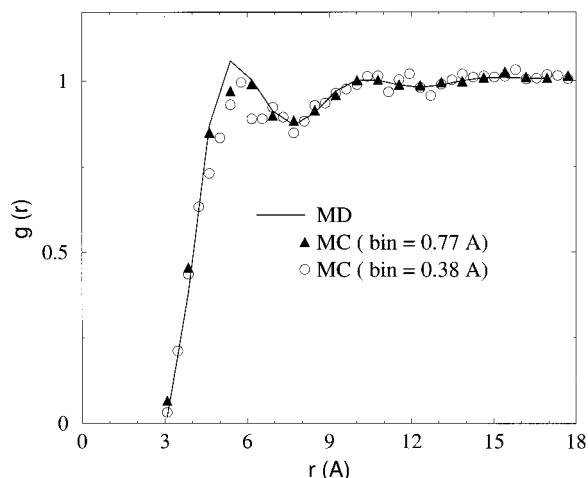


Figure 2. Comparison of the lattice derived intermolecular pair distribution function for C_{31} chains to that derived from molecular dynamics simulations under saturated liquid conditions at $T = 423$ K.

$T = 423$ K. Figure 2 compares the $g(r)$ calculated with two different bin sizes of $\Delta r = 0.77$ Å and 0.38 Å. It is clear that the lattice calculations and the off-lattice simulations are in quantitative agreement for $r > 6$ Å, especially for the bin size of 0.77 Å. The disagreement at shorter distances, which is outside the uncertainties in the simulations (typically the size of the points), is probably caused by the fact that bond angles are fixed in the lattice calculations. Note that particular care must be taken in the choice of the bin variable, Δr , for comparing the $g(r)$'s. Picking too small a value of this quantity will cause the lattice results to acquire peaks and valleys associated with the discretization. To quantify the consequences of the small discrepancies in the pair distribution functions, we computed the cohesive energy density for C_{31} using equilibrated configurations obtained from both MD and lattice MC at $T = 423$ K. The cohesive energy density is defined as the square root of the ratio of the enthalpy of vaporization and the molar volume of the saturated liquid phase. The values obtained from MD and lattice MC were 181 and 178 MPa, respectively, showing that the errors observed in $g(r)$ do not have measurable consequences on the properties we have measured. Figure 3 compares the

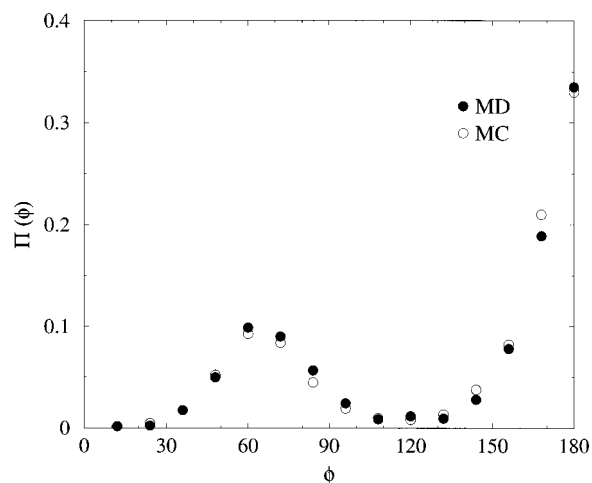


Figure 3. Comparison of lattice-derived torsion angle distribution for C_{31} chains to that derived from molecular dynamics simulations under saturated liquid conditions at $T = 423$ K.

distribution of torsional angles at the same state conditions. Again, remarkably good agreement is obtained between the lattice and off-lattice simulations. These results show that the lattice approximation introduces little error when compared to the full off-lattice calculation.

An important issue is the speed-up afforded by employing a lattice, which originates primarily in the calculation of the potential energy (i.e., the Lennard-Jones interactions and torsion). For an unoptimized simulation, the net speed-up is

$$\frac{\frac{n^2}{2}t_{LJ}^{\text{off-lat}} + nt_{\text{torsion}}^{\text{off-lat}} + nt_{\text{overhead}}}{\frac{n^2}{2}t_{LJ}^{\text{lat}} + nt_{\text{torsion}}^{\text{lat}} + nt_{\text{overhead}}}$$

where n is the number of monomers in the system, and t_{overhead} accounts for all of the simulation expenses, excluding the calculation of the potential energies. This overhead is normally small and can be ignored relative to the other two terms. t_{LJ} and t_{torsion} correspond to the times required for a *single* Lennard-Jones and a torsion angle potential calculation. The superscripts “lat” and “off-lat” refer to the lattice and off-lattice model, respectively. We find $t_{LJ}^{\text{off-lat}}/t_{LJ}^{\text{lat}} \sim 10$, in agreement with published results,⁵ $t_{\text{torsion}}^{\text{off-lat}}/t_{\text{torsion}}^{\text{lat}} \sim 50$, and $t_{\text{torsion}}^{\text{lat}}/t_{LJ}^{\text{lat}} \sim 1$, independent of ζ in the range 5–25. Since $n = 1000$ –5000 in a typical saturated liquid simulation, it is clear that the Lennard-Jones calculation is the dominant factor in these simulations. Thus, speed-ups of order 10 are expected and are found for example in the simulation of the vapor–liquid coexistence for hexadecane. Similarly, we performed a grand canonical ensemble simulation for hexane, at $T = 0.7T_c$, and watched the system evolve from an initial density corresponding to the critical density to its liquidlike value. Again, a speed-up of 10 was found in going to the lattice calculation. Improvements, such as the use of a link list for enumerating the number of Lennard-Jones neighbors, will reduce the number of dispersive interactions to $(n/2)t_{LJ}$ in both the lattice and off-lattice cases, but with large prefactors (~ 100) which account for the number of neighbors expected in a typical dense liquid. This will result in a small additional speed-up of order 10–20%.

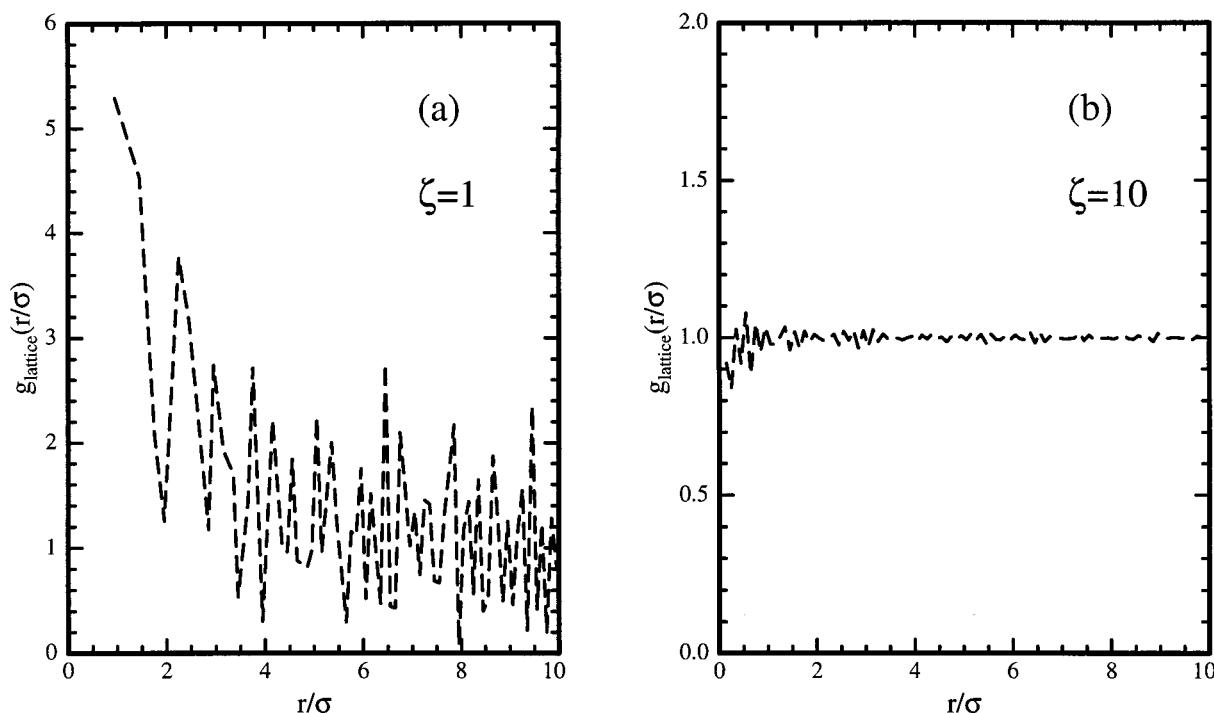


Figure 4. Plot of the lattice pair distribution function, $g_{\text{lattice}}(r)$, as defined in the text for two different lattices: (a) $\zeta = 1$ and (b) $\zeta = 10$. Both plots were obtained for the same bin size $\Delta r/\sigma = 0.2$.

Thus, we generically find speed-ups of order 10 when one models polymer liquids with real structure and interactions on a lattice. Of course, significant speed-ups are expected for dilute gas phases, where in the $n \rightarrow 0$ limit, one expects a speed-up of order 50, especially if link lists are utilized.

At this juncture it is crucial to examine the reasons for the excellent agreement between the off-lattice calculations and the lattice approximation for three separate cases, the Lennard-Jones fluid,⁵ the restricted primitive model,⁴ and the long-chain *n*-alkanes. This analysis will also provide a rationale for selecting an appropriate ζ for the accurate simulation of any model using a fine-grained lattice. To get an accurate representation of the thermodynamics of an off-lattice system by utilizing these lattice ideas requires that the system free energy, F , be properly reproduced. Since $F = U - TS$, the energy, U , and the entropy, S , must be independently well represented. The total internal energy is the sum of the intramolecular and intermolecular energies. The intramolecular energy involves the bond angle and torsional energies. We have fixed the bond angle to the equilibrium value in our simulation. Also, the torsion angle distribution and hence torsional energies in our simulation match precisely with the off-lattice simulation. By elimination, the only unaccounted errors are in the calculation of the Lennard-Jones or the dispersive part of the energy. The dispersive part of the internal energy of the system is defined exactly by the equation $U \equiv 2\pi \int_0^\infty r^2 g(r) u(r) dr$. Similarly, the entropy of the system can be described at the level of the two-body approximation as $S \sim \int_0^\infty g(r) \ln g(r) d^3r$. We consider the effect of lattice discretization on U as an illustrative example. The spatial discretization induced by the use of a lattice introduces two possible inaccuracies: (a) the intermolecular packing, or the radial distribution function, $g(r)$, is not properly modeled, and (b) the potential energy well is not sampled properly, especially near the minimum.

To understand the importance of these two issues, consider the case of a cubic lattice with $\zeta = 1$. The smallest separation between two lattice points is the atomic diameter, $r/\sigma = 1$, with a coordination number $z = 6$. (Here σ is the segment size.) The next separation distance is $\sqrt{2}$, with $z = 12$. Thus, the lattice only allows for certain discrete separations to be accessed (point (a) above). Moreover, for this ζ , the Lennard-Jones minimum at $2^{1/6}\sigma$ is not sampled adequately (point (b) above). In combination, both of these factors yield a poor estimate for U . As ζ increases, the range of accessible separation distances, especially for relevant r/σ , approaches a continuum. To quantify the difference between the lattice and continuum, we define the lattice density, $g_{\text{lattice}}(r)$, $n_{\text{lattice}}(r) dr = 4\pi r^2 g_{\text{lattice}}(r) dr$, where $n_{\text{lattice}}(r)$ is the number of lattice placements in a shell of width dr located a distance r from the origin. Since $g_{\text{lattice}}(r) = 1$ for all relevant r as $\zeta \rightarrow \infty$, departures of g_{lattice} from 1 represent the errors induced by lattice discretization. For the sake of comparison to the intermolecular $g(r)$ values presented in Figure 2, we use the same $\Delta r = 0.77$ Å. The results for $\zeta = 1$ and $\zeta = 10$ are shown in Figure 4. Clearly, increasing ζ causes the lattice discretization effects to be hidden within the hard core (i.e., $r/\sigma < 0.8$). This analysis shows that the lattice packing closely resembles its off-lattice analogue even for $\zeta = 10$.

To assess the effect of lattice discretization on system thermodynamics, we calculate the energy of a lattice fluid interacting through a Lennard-Jones potential in the van der Waals approximation. Thus, we assume that molecular packing follows the bulk density except for constraints imposed by the spatial discretization of the lattice. In addition, the calculation of energy is affected by the discrete values of r which can be sampled by the lattice. Thus, we place one molecule at the origin and sample all possible positions on the lattice that the second particle can access. Using this procedure, for the case of $\zeta = 1$, we find that $U_{\text{lattice}}/U_{\text{off-lattice}} = 0.73$, while for $\zeta = 5$ and 10, it becomes respectively 1.008 and

0.995, independent of density. ($U_{\text{off-lattice}}$ is the energy obtained from an off-lattice fluid in the van der Waals approximation.) Our results suggest that $\zeta = 5$ is sufficient to reproduce off-lattice results for system energy. These conclusions are consistent with our findings that ethane, the restricted primitive model⁴ and the Lennard-Jones atomic fluid,⁵ can be modeled accurately with $\zeta = 5$. In contrast, for the longer alkanes we employed $\zeta = 12$ so as to accommodate the constraints of bond length and bond angle. In all of these cases, it is straightforward to estimate the minimal ζ necessary to reproduce the off-lattice results.

Finally, we stress the generality of these ideas to the simulations of any polyolefin. Since this class of polymers, except poly(isobutylene), is described by the same set of bond lengths, bond angles, and torsional potentials, they can be modeled by the same $\zeta = 12$. PIB is unusual since it incorporates two different bond angles, 109.5° and 122°. In this case a larger $\zeta = 20$ needs to be employed. We stress here that, since all our computations are independent of the value of ζ in the range 5–25, the speed-ups of these calculations are expected to be of order 10 in all cases. Finally, if one chose to consider explicit atom descriptions, then a $\zeta = 18$ will be necessary to incorporate the tetrahedral bond angles and also the relatively short C–H bond (1.1 Å).

Our results suggest that a paradigm shift is in order. It appears unnecessary, on the basis of the data from the Lennard-Jones monomer fluid, the restricted primitive model, and the hydrocarbon chains, to sample phase space in all of the detail afforded by an off-lattice calculation. Rather, a much more coarse-grained lattice approach is sufficient to quantitatively model the phase behavior and the structure of these chain fluids. While not sacrificing accuracy, the lattice approach permits for simulations that are 10–100 times cheaper than the

off-lattice analogues, thus permitting us to perform simulations that are inaccessible by any other currently available technique.

Acknowledgment. Funding was provided by the National Science Foundation (DMR-9804327, CTS-9975625 A.I., S.K.K.) and the Department of Energy (DE-FG02-98ER14858, A.Z.P.).

References and Notes

- (1) Nath, S.; Escobedo, F.; dePablo, J. J. *J. Chem. Phys.* **1998**, *108*, 9905.
- (2) Lohse, D. J.; Datta, S. *Polymeric Compatibilizers*; Hanser Publishers: Cincinnati, OH, 1996.
- (3) Yan, Q.; dePablo, J. J. *J. Chem. Phys.* **2000**, *113*, 5954.
- (4) Panagiotopoulos, A. Z.; Kumar, S. K. *Phys. Rev. Lett.* **1999**, *83*, 2981.
- (5) Panagiotopoulos, A. Z. *J. Chem. Phys.* **2000**, *112*, 7132.
- (6) Smit, B.; Karaborni, S.; Siepmann, J. I. *J. Chem. Phys.* **1995**, *102*, 2126.
- (7) Allen, M. P.; Tildesley, D. J. *Computer Simulations of Liquids*; Oxford University Press: New York, 1986.
- (8) MacDonald, I. R.; Singer, K. *Discuss. Faraday. Soc.* **1967**, *43*, 40.
- (9) Alves, N. A.; Berg, B. A.; Villanova, R. *Phys. Rev. B* **1990**, *41*, 383.
- (10) Ferrenberg, A. M.; Swendsen, R. H. *Phys. Rev. Lett.* **1988**, *61*, 2635.
- (11) Ferrenberg, A. M.; Swendsen, R. H. *Phys. Rev. Lett.* **1989**, *63*, 1195.
- (12) Wilding, N.; Muller, M.; Binder, K. *J. Chem. Phys.* **1996**, *105*, 802.
- (13) Deutsch, H.-P. *J. Stat. Phys.* **1992**, *67*, 1039.
- (14) Deutsch, H.-P. *J. Chem. Phys.* **1993**, *99*, 4825.
- (15) Panagiotopoulos, A. Z.; Wong, V.; Floriano, M. A. *Macromolecules* **1998**, *31*, 912.
- (16) Frenkel, D.; Smit, B. *Understanding Molecular Simulation*; Academic Press: New York, 1996.
- (17) Flory, P. J. *Principles of Polymer Chemistry*; Cornell University Press: Ithaca, NY, 1953.

MA011379S